

An Attempt to Infer Flow Patterns and Tectonic Styles from the Gradient of Two-Dimensional GPS Velocity Fields

Bob Simpson - Draft

October 16, 2016

Abstract

Deformation and flow styles are commonly described in a qualitative way by words such as “shear, convergence, extension.” Folks exposed to a structural geology class or a rock mechanics class have experienced a more explicit vocabulary containing terms such as “oblique right-lateral shear with extension.” Disregarding the intensity and orientation or the deformation, we propose a scheme for parameterizing deformation styles using two angles inferred from the gradient tensor and for plotting on an equal area (Schmidt) net. We offer a plausible way of dividing the net into 17 discrete, named domains.

1 Introduction

This began as an effort to visualize deformation styles, ideally in a colored map view, given a regional GPS velocity field. The usual plots of dilatation, rotation, and other derived strain parameters can help, but such plots individually tell only part of the story and tend to give simple shear somewhat short shrift. It seemed that there might be a better way to characterize the velocity field in the neighborhood of a point using some nomenclature for common deformation styles. For context, it’s useful to consider the related problem of characterizing the kinematics of fluid flow — think “vorticity” instead of “rotation” and “shear” instead of “strike-slip” (e.g., Batchelor, 1967).

It turns out that the information needed is available in the gradient of the vector field.

2 The gradient and the gradient tensor (GT)

The gradient of a two dimensional velocity field $\vec{v}(\vec{x})$ can be written as a tensor (matrix) in a chosen x,y coordinate system. For example, with $u(x, y)$ and $v(x, y)$ being the east and north components of a GPS velocity field in the x- and y-axis directions:

$$GT = \begin{bmatrix} \partial u / \partial x & \partial u / \partial y \\ \partial v / \partial x & \partial v / \partial y \end{bmatrix} = \begin{bmatrix} a & b \\ c & d \end{bmatrix} \quad (1)$$

As will be seen, the collection of gradient tensors can be thought of as a 4-dimensional vector space, which leads to some interesting geometric insights. (The letters a, b, c, d will be used in what follows to simplify expressions involving components of the gradient tensor.)

In infinitesimal strain analysis, it is common to partition the gradient tensor into an antisymmetric **rotation** (vorticity) tensor and a symmetric **strain** tensor (e.g., Jaeger, 1969):

$$GT = \begin{bmatrix} \partial u / \partial x & \partial u / \partial y \\ \partial v / \partial x & \partial v / \partial y \end{bmatrix} = \begin{bmatrix} 0 & -\omega \\ \omega & 0 \end{bmatrix} + \begin{bmatrix} \varepsilon_{xx} & \varepsilon_{xy} \\ \varepsilon_{xy} & \varepsilon_{yy} \end{bmatrix} \quad (2)$$

where $\omega = \frac{1}{2}(\frac{\partial v}{\partial x} - \frac{\partial u}{\partial y})$, $\varepsilon_{xx} = \frac{\partial u}{\partial x}$, $\varepsilon_{xy} = \varepsilon_{yx} = \frac{1}{2}(\frac{\partial v}{\partial x} + \frac{\partial u}{\partial y})$, $\varepsilon_{yy} = \frac{\partial v}{\partial y}$.

Deformation related to a **change in size** can also be separated from that related to **change in shape** by resolving the strain tensor in Equation (2) into the sum of an isotropic tensor and a traceless *pure shear* tensor with no change in size (area):

$$GT = \begin{bmatrix} 0 & -\omega \\ \omega & 0 \end{bmatrix} + \frac{\Delta}{2} \begin{bmatrix} 1 & 0 \\ 0 & 1 \end{bmatrix} + \begin{bmatrix} \varepsilon_{xx} - \frac{\Delta}{2} & \varepsilon_{xy} \\ \varepsilon_{xy} & \varepsilon_{yy} - \frac{\Delta}{2} \end{bmatrix} \quad (3)$$

where dilatation $\Delta \equiv \varepsilon_{xx} + \varepsilon_{yy}$.

Because the pure shear tensor (the last term in Equation 3) is symmetric, it can be diagonalized by a change of coordinate axes (a new x,y coordinate system) defined by its principal axes. A quick calculation (Appendix A) shows that the form of the rotation-vorticity and size-change tensors (the first and second terms in Equation 3) remains unchanged under the transformation to the new principal-axis coordinate system. (This 'rotation' of coordinate systems should not be confused with the rotation-vorticity component of the gradient tensor!) In the new coordinate system:

$$GT = \begin{bmatrix} 0 & -\omega \\ \omega & 0 \end{bmatrix} + \frac{\Delta}{2} \begin{bmatrix} 1 & 0 \\ 0 & 1 \end{bmatrix} + \begin{bmatrix} e & 0 \\ 0 & -e \end{bmatrix} = \omega \begin{bmatrix} 0 & -1 \\ 1 & 0 \end{bmatrix} + \frac{\Delta}{2} \begin{bmatrix} 1 & 0 \\ 0 & 1 \end{bmatrix} + e \begin{bmatrix} 1 & 0 \\ 0 & -1 \end{bmatrix} \quad (4)$$

where e and $-e$ are the eigenvalues (with $e \geq 0$ being the larger of the two). The eigenvalues are necessarily equal and opposite since the trace must still sum to zero (the trace is invariant under changes in coordinate system). The usual calculation for eigenvalues gives $e = \frac{1}{2}\sqrt{(a-d)^2 + (c+b)^2}$.

Thus, the gradient tensor has been transformed to three parameters multiplying three matrices with simple interpretations, plus a rotation angle specifying the relation of the new coordinate system relative to the old.

3 Basis vectors for the 4-dimensional GT space

If we think of the gradient tensor as a vector $[a, b, c, d]$ in a 4-dimensional vector space, then equation (4) suggests that a natural basis for this vector space for deformation investigations might be: $[0, -1, 1, 0]$, $[1, 0, 0, 1]$, $[1, 0, 0, -1]$, $[0, 1, 1, 0]$. The first three of these vectors have been identified above as rotation (vorticity), size-change (dilatational), and shape-change (pure shear). The last vector is also a pure shear (it's symmetric, so it can be diagonalized) but its principal axes are oriented at 45° to those of the third basis vector. Thus the hyper-plane in the 4-dimensional space spanned by the last two vectors contains all possible pure shear combinations. This proposed basis is orthogonal using the usual scalar product (but not orthonormal since all of the vectors all have length $\sqrt{2}$). Examples of the motions/deformations expected from the gradient tensors associated with these basis vectors are shown in **Figure 1**.

A more usual choice of basis for a 4-dimensional vector space would be the set of vectors $[1, 0, 0, 0]$, $[0, 1, 0, 0]$, $[0, 0, 1, 0]$, $[0, 0, 0, 1]$, and it turns out that these also have simple tectonic styles associated with them. For example, the first of these vectors represents uniaxial extension parallel to the x-axis, and the second describes right-lateral (RL) simple shear parallel to the x-axis. **Figure 2** illustrates the motions expected from this set of basis vectors. Note, for example, that the simple shear $[0, 0, 1, 0]$ is spanned by and is a linear combination of a rotation $[0, -1, 1, 0]$ and a pure shear $[0, 1, 1, 0]$.

The initial set of basis vectors proposed in the first paragraph of this section offers a way to re-parametrize the information in the GT: Equation (4), suggests that we can replace the 4 GT components a, b, c, d with four new parameters $\omega, \frac{\Delta}{2}, e$, and an angle β specifying the orientation of the new x', y' principal axis coordinate frame relative to the original x, y coordinate frame. If we are mostly interested in the style of deformation and not necessarily in its orientation, we can ignore the angle β , leaving a 3-dimensional vector $[A, B, C] = [\omega, \frac{\Delta}{2}, e]$, which may be slightly easier to visualize. In fact, since we chose $e \geq 0$, to be the larger eigenvalue, the vectors $[A, B, C]$ are confined to the upper half-space, with:

$$A = \frac{1}{2}(c - b), \quad B = \frac{1}{2}(a + d), \quad C = \frac{1}{2}\sqrt{(a - d)^2 + (c + b)^2} \quad (5)$$

A further simplification is possible, if we're only interested in the style of motion/deformation and not its intensity or magnitude. Let the magnitude of the GT be defined to be the length of the corresponding 4-dimensional vector: $mag(GT) = \sqrt{a^2 + b^2 + c^2 + d^2} = \sqrt{A^2 + B^2 + C^2}$. Then normalizing the 3-dimensional vectors $[A, B, C]$ vectors by their lengths yields a hemisphere of unit radius in the 3-dimensional upper halfspace, and each $[A, B, C]$ vector has been normalized and turned into a direction piercing the hemisphere. Using an old trick long employed by structural geologists, this hemisphere can be mapped onto a plane piece of paper using an equal-area (Schmidt) net or projection). This projection, which preserves area, is also known as a Lambert Azimuthal Equal Area projection (e.g., Wikipedia).

We note in passing that information about non-rigid deformation (i.e., change of size, change of shape) is contained in components B and C , so a measure of the non-rigidity should be $\sqrt{B^2 + C^2}$. (This quantity is a multiple of the so-called *second invariant* of the strain tensor (e.g., Kreemer et al., 2015)). It follows that the tectonic styles (flow patterns) proposed in the next section include not just deformation information (B and C), but also reference frame information (A). As in plate tectonics, rigid plates can be viewed from different reference frames rotation relative to each other, and the rotation/vorticity parameter (A) will change in these different frames. (See Appendix B for more on this subject.)

4 Classification of the motion/deformation styles

Obviously, each $[A, B, C]$ corresponds to a deformation style. Here is a list of selected common styles by name, along with corresponding $[A, B, C] = [\omega, \frac{\Delta}{2}, e]$ values, normalized to one. [Help: are there better lists or better names?] A longer list of examples of gradient tensor $[a, b, c, d]$ values leading to these categories is given in Appendix C.

1. $[A, B, C] = [\pm 1, 0, 0]$: Rotation CCW/CW
2. $[A, B, C] = [0, \pm 1, 0]$: Uniform expansion/contraction (size change)
3. $[A, B, C] = [\pm \frac{1}{\sqrt{2}}, \pm \frac{1}{\sqrt{2}}, 0]$: Vortex, swirling with CCW/CW rotation \pm Expansion/Contraction
4. $[A, B, C] = [0, 0, 1]$: Pure Shear (shape change)
5. $[A, B, C] = [\pm \frac{1}{\sqrt{2}}, 0, \frac{1}{\sqrt{2}}]$: Simple Shear RL/LL
6. $[A, B, C] = [0, \pm \frac{1}{\sqrt{2}}, \frac{1}{\sqrt{2}}]$: Uniaxial extension/convergence
7. $[A, B, C] = [\pm \frac{1}{2}, \pm \frac{1}{2}, \frac{1}{\sqrt{2}}]$: Oblique extension/convergence with RL/LL
8. infinite gradations of the above, from one category to adjacent ones...

The oblique styles are linear combinations of a simple shear (e.g., $[a, b, c, d] = [0 \ 1 \ 0 \ 0]$) and a uniaxial extension or convergence (e.g., $[a, b, c, d] = [1 \ 0 \ 0 \ 0]$), yielding a combined deformation (e.g., $[a, b, c, d] = [1, 1, 0, 0]$ with $[A, B, C] = [\frac{1}{2}, \frac{1}{2}, \frac{1}{\sqrt{2}}]$). Thus the reference oblique styles here (item 7 in the list) have equal amounts of simple shear and extension/convergence, although the term oblique as commonly used does not have any fixed proportion of the two components.

5 Viewing styles on an equal-area plot

Figure 3 shows a mapping of the unit-hemisphere in the upper $[A, B, C]$ half-space to an equal area net. In this figure, the A value (rotation-vorticity) has been assigned to the x-axis of the net, the B value (size-change) to the y-axis of the net, and C (pure shear = shape change) to the center of the net (the zenith). The various selected categories of styles listed in the previous section are separated with dotted lines and by color on the plot. The first two categories, size change and rotation, fall at the edges of the map (the A - B plane), the third, shape change, falls at the center of the net. Other categories are centered within dotted compartments with their names attached. Thus, for example, the case named “RL Simple Shear” falls in the center of a region labeled with that name. Other points in that region are *mostly* “RL Simple Shear”, but grade with increasing amounts of convergence, extension, rotation, or pure shear into adjacent regions depending on direction. For the oblique categories, UC/RL implies a combination of Uniaxial Convergence and RL shear.

Coloring this plot using a continuous color wheel initially seemed like an obvious choice. The results, although aesthetically pleasing, tended to be confusing and even somewhat mind-blowing. Discrete color steps seemed a better way to go after some experimentation. As will be seen in the examples that follow, different study areas contain different tectonic environments and a color scheme appropriate for one study area may not be optimal for others.

So far, in pursuing styles we have ignored the magnitude of the gradient vector. One way to view this on a map, already colored by styles would be to display contours of the gradient magnitude. (An experiment trying to use color saturation to indicate intensity of deformation also proved confusing given the large number of colors and shades involved.) An alternative approach used in some map examples in the next section is to show several plots with a succession of lower and lower threshold values for the magnitude. [Ideally, viewing might be best done interactively with a program that would allow thresholds to be changed and colors to be altered to optimally reveal the tectonics of the region under study.]

6 Example plots for Western US

Gradient tensors can be calculated either from east and north velocities interpolated to a regular rectangular mesh, or from a Delaunay triangulation of observation sites. The first approach yields a gradient tensor at every grid point in the mesh. The second, a gradient tensor for every triangle in the triangulation.

Figure 4 was made using grids of the WUS compilation of western US GPS velocity observations kindly provided by Rob McCaffrey. The north and east velocity observations were interpolated to grids using a minimum curvature algorithm and slightly smoothed by an upward continuation filter. The gradient tensor at each grid point was calculated from the grids by numerical differentiation. (See Simpson and Thatcher, 2016, in preparation.)

On the left is an equal-area plot showing styles and on the right and a map view of locations for which the gradient tensors had magnitudes greater than 0.25 microstrain. Not surprisingly, most tensors with such relatively large magnitudes are located along the San Andreas fault in California. Note a region of light blue north of the Mendocino Triple Junction in California exhibiting mostly clockwise vorticity, and also a small green region in Mexico of oblique UE/RL extension (best regarded with some skepticism given its location near the edge of the grid).

Figure 5 is a similar plot, showing gradient tensors with magnitudes greater than 0.04 microstrain. Note regions of oblique RL convergence along the coasts north of the Mendocino Triple Junction, changing northward in northwest Washington to convergence, oblique LL convergence, and LL shear in the vicinity of Vancouver Island. (The last style is at the edge of the map area – one must in such cases be suspicious of gridding edge effects.) The white area in Central California bounded by RL shear on the San Andreas fault system to its west and by more RL shear in the Eastern California shear zone (ECSZ) to its east, coincides with the Sierra-Nevada microplate, which is encircled by earthquakes, but largely avoided by earthquakes within the apparently sturdy microplate. Spots of green along the ECSZ suggest a component of extension in this RL shear zone. Near the Mendocino Triple Junction, light blue regions of CW rotation surround a slightly darker blue region have components of CW rotation and contraction. A similar small region in the Central Oregon coast is of the same color, again suggesting rotation plus contraction.

Figure 6 shows a grid of selected data from Snay et al. (2016) excluding only regions with no data within 100 km. Throwing caution to the winds, no attempt has been made in this plot to blank out areas with low intensities of deformation or to attempt to propagate uncertainties. MMDD/mMDD deformation symbols are not scaled by the magnitude of the gradient tensor. Black lines in the symbols show MMDD, white lines show the mMDD part. The LL shear colors in Utah and southern Nevada lying along the margin of the Colorado Plateau coincide with the Pahranagat shear zone, a SW trending LL zone accommodating westward extension in the Basin Range province (per Ray Wells). Note also the LL simple shear on Vancouver Island opposite the Nootka fracture zone offshore.

Figure 7 shows a Delaunay triangulation of selected data from Snay et al. (2016). In this case, an attempt was made to propagate the uncertainties in the reported velocity observations, first by calculating a gradient tensor for each triangle and propagating the uncertainties in the velocity observations into (uncorrelated) uncertainties for each of the four components of the gradient tensor. For each component, we have 3 quantities: the original estimate of the component and the estimates at +/- one standard deviation. This yields 81 realizations of the gradient tensor for each triangle, and 81 estimates of the style. One can plot the locations of the suite of styles on an equal area plot. Ideally if the uncertainties are small, these points will form a small tight cluster. However, triangles with very low velocities, but moderately large velocity uncertainties at each corner, can offer a wide variety of styles, mostly of no particular significance. One restraint on the tightness of the cluster is offered by the number of styles estimated. Requiring only one style of all realizations is a bit restrictive, because the styles may occur near a boundary between two boxes in Figure 3, or near a corner abutting four discrete named styles. For this figure, we have colored only those triangles with 4 or fewer styles in their suite of styles. (Another discriminant might be an angular measure of the diameter of the cluster of styles.)

Figure 8 ignores the change in scale (dilatation) style dimension and uses a different coloring of styles than in previous figures — more continuous than discrete — across a horizontal cross-section of the [A,B,C] upper hemisphere. Shading is intended to indicate the magnitude of the deformation, with the idea that small deformations are less likely to yield significant style picks. MMDD/mMDD symbols are scaled to the magnitude of the deformation. Data are from the WUS compilation of velocities of Rob McCaffrey.

Figure 9 ignores the rotation (vorticity) style dimension and uses a different coloring of styles than in previous figures across a vertical cross-section of the [A,B,C] upper hemisphere. Shading is intended to indicate the magnitude of the deformation, with the idea that small deformations are less likely to yield significant style picks. Data are from the WUS compilation of velocities of Rob McCaffrey.

7 Things that still need attention...

Propagation of uncertainties through the gridding process still needs to be addressed. One way around this is to use a Delaunay triangulation of the area of interest, with triangles formed from triples of observations. Each observation has known uncertainties, and each triangle yields an $[a, b, c, d]$ deformation matrix with each component having a propagated uncertainty. These uncertainties can be carried through the equal-area projection process, resulting in an error ellipse that could be plotted on the equal-area net around each point, giving some impression as to the reality of the style assignment.

The question of optimal reference frame for a given study area was left unresolved. As mentioned in Appendix B, the choice of reference frame has an effect (hopefully small in most cases) on the inferred style. For a really simple example, imagine the Earth's surface covered by two plates rotating past each other in strike-slip fashion with respect to each other with a finite width shear zone between the plates. Three reference frames stand out as useful possibilities: Plate A fixed, Plate B fixed, or both plates treated more equally by using the half-pole reference frame of Wdowinski and Shen (Wdowinski, 2007). But what about 3 plates? What are the optimal reference frames in this case?

Are there better classification of tectonic styles available? I've looked through several structural geology text books and searched with Google for systematic schemes for organizing tectonic styles. It seems likely, given that structural geologists have been stamping around for probably 300+ years now, that there have been other attempts at classifications. Any ideas?

And, of course, the ultimate questions: Does this make any sense? Is this good for anything?

Comments, criticisms, and suggestions would be appreciated as always!

References

- [1] Batchelor, G.K., 1967, An Introduction to Fluid Dynamics. Cambridge University Press, 615 p.
- [2] Jaeger, J.C., 1967, Elasticity, Fracture and Flow: With Engineering and Geological applications: Methuen & Co. Ltd., 268 p.
- [3] Kreemer, C., Blewitt, G., and Klein, E.C., 2014, A geodetic plate motion and Global Strain Rate Model: *Geochem. Geophys. Geosyst.*, 15, 3849-3889, doi:10.1002/2014GC005407.
- [4] McCaffrey, R., 2005, Block kinematics of the Pacific–North America plate boundary in the southwestern United States from inversion of GPS, seismological, and geologic data: *Jour. Geophys. Res.*, v. 110, p. B07401, doi:10.1029/2004JB003307.
- [5] McCaffrey, R., King, R., Payne, S.J., Lancaster, M., 2013, Active tectonics of northwestern U.S. inferred from GPS-derived surface velocities: *Journal of Geophysical Research*, v.118, p.709-723, doi:10.1029/2012JB009473.
- [6] Simpson, R., and Thatcher, W., 2016, A method for detecting gradients in regional GPS velocity fields to locate and characterize features of tectonic interest: (draft).
- [7] Snay, R.A., Freymueller, J.T., Craymer, M.R., Pearson, C.F., Saleh, J., 2016, Modeling 3-D crustal velocities in the United States and Canada: *Journal of Geophysical Physics*, 15 July 2016, DOI: 10.1002/2016JB012884.
- [8] Wdowinski, Shimon, Smith-Konter, B., Bock, Y., Sandwell, D., 2007, Diffuse interseismic deformation across the Pacific-North America plate boundary, *Geology*, v. 35, p. 311-314, doi: 10.1130/G22938A.
- [9] Wikipedia, 2016.

Appendix A - Eigenvalues and Transformation to Principal Axes Coordinate Frame

Using letters a, b, c, d for convenience, and partitioning into scale-change, rotation, and pure shear components

$$GT = \begin{bmatrix} a & b \\ c & d \end{bmatrix} = \frac{1}{2}(a+d) \begin{bmatrix} 1 & 0 \\ 0 & 1 \end{bmatrix} + \frac{1}{2}(c-b) \begin{bmatrix} 0 & -1 \\ 1 & 0 \end{bmatrix} + \begin{bmatrix} P & Q \\ Q & -P \end{bmatrix} \quad (6)$$

where $P = (a - d)/2$ and $Q = (c + b)/2$. Eigenvalues for the last matrix are found by solving the determinant equation: $(P - e)(-P - e) - Q^2 = 0$, so that the eigenvalues are: $e = \pm\sqrt{P^2 + Q^2} = \pm\frac{1}{2}\sqrt{(a - d)^2 + (c + b)^2}$. The principal axis x',y' coordinate system is oriented at an angle β relative to the original x,y coordinate system.

Changing the GT to the principal axis coordinate system involves a coordinate-system rotation. A general rotation through an angle β is of the form:

$$R(\beta) = \begin{bmatrix} \cos\beta & -\sin\beta \\ \sin\beta & \cos\beta \end{bmatrix} \quad (7)$$

Applying this rotation matrix to a vector (x,y) will give its coordinates in a the new rotated axis system. The rule to convert a tensor (a linear transformation matrix) T to the new coordinate system is: $M' = R(\beta) M R(\beta)^t$ where the last term is the transpose of the rotation matrix.

A useful observation that can be confirmed by a simple calculation is that matrices of these two forms do not change regardless of angle β :

$$\begin{bmatrix} 1 & 0 \\ 0 & 1 \end{bmatrix}, \quad \begin{bmatrix} 0 & -1 \\ 1 & 0 \end{bmatrix} \quad (8)$$

Appendix B - Note on frames of reference

It's worth mentioning that the rotational-vorticity component expressed in component A is rigid in the sense that the distances between points are preserved if $B = C = 0$. Thus the A component does contribute to the flow or motion in the chosen frame of reference, but doesn't contribute to shape distortion.

One obvious question might be: "Why not convert to a rotating frame of reference, as is frequently done in plate tectonic calculations on the surface of the earth, so that there is no rotation component — so $A = 0$? But will a single frame of reference work for all points? Thinking of the fluid flow analog with small vortices related to turbulence, it's not clear what the optimal frame of reference might be. Similarly, Myrl Beck and others have proposed from paleomagnetic observations the idea that in a regional strike-slip environment there exist isolated blocks (Beck's ball bearings) that rotate in the shear zone. Again, what's the optimal frame of reference for the study region as a whole? Finally, in a finite width shear zone with two plate sliding past each other, each point in the shear zone has an A component that could be canceled out in an appropriate rotating reference frame, but each point in the shear zone requires a different rotating frame (i.e. different center of rotation), and any one of these would make the whole shear zone itself rotate, which doesn't seem desirable.

So how does one choose an optimal reference frame for a give study area? It seems clear that different rotating reference frames will change the A value, and hence the assigned tectonic style. Maybe for any reasonable choice of reference frame for a given geologic study area, the changes in A will be small compare to the magnitude of A . (Any thoughts on this subject of reference frames would be greatly appreciated!)

Appendix C - Examples of gradient tensors in the various categories.

In the mapping from $[a, b, c, d] \rightarrow [A, B, C]$, any orientation information in the form of the principal axis directions has been lost. Given an $[A, B, C]$ vector it is possible to recover a "sample" GT of the sort that would have produced this vector by using equation (4) and substituting $[A, B, C] = [\omega, \frac{\Delta}{2}, e]$. This sample is not the only GT that would have produced the given $[A, B, C]$ vector, but the full collection of GT's can be produced by rotating the coordinate system this sample using the formula in Appendix A.

Here are sample GT tensors for each of the proposed tectonic-style categories:

- Uniform expansion: $[1,0,0,1]$ (in any x,y coordinate system) $\rightarrow (A,B,C) = (0,1,0)$
- Uniform contraction: $[-1,0,0,-1]$ (in any x,y coordinate system) $\rightarrow (A,B,C) = (0,-1,0)$
- CCW Rotation: $[0,-1,1,0]$ (in any x,y coordinate system) $\rightarrow (A,B,C) = (1,0,0)$
- CW Rotation: $[0,1,-1,0]$ (in any x,y coordinate system) $\rightarrow (A,B,C) = (-1,0,0)$

- Pure shear: $[1,0,0,-1]$ (extension parallel to x-axis, contraction parallel to y-axis) $\rightarrow (A,B,C) = (0,0,1)$
- Pure shear: $[\cos 2\theta, \sin 2\theta, \sin 2\theta, -\cos 2\theta]$ (extension in direction θ measured CCW from x-axis, contraction perpendicular)
- Pure shear: $[-1,0,0,1]$ (extension parallel to y-axis, contraction parallel to x-axis)
- Pure shear: $[0,1,1,0]$ (extension at 45-degrees, contraction at 135-degrees)
- Pure shear: $[-\sin 2\theta, \cos 2\theta, \cos 2\theta, \sin 2\theta]$ (extension in direction $\theta + 45^\circ$ measured CCW from x-axis, contraction perpendicular)
- Pure shear: $[0,-1,-1,0]$ (extension at 135-degrees, contraction at 45-degrees)
- Uniaxial extension: $[1,0,0,0]$ (parallel to x-axis)
- Uniaxial extension: $[0,0,0,1]$ (parallel to y-axis)
- Uniaxial extension: $[\cos^2 \theta, \sin \theta \cos \theta, \sin \theta \cos \theta, \sin^2 \theta]$ (in direction θ measured CCW from x-axis)
- Uniaxial convergence: $[-1,0,0,0]$ (parallel to x-axis)
- Uniaxial convergence: $[0,0,0,-1]$ (parallel to y-axis)
- RL simple shear: $[0,1,0,0]$ (parallel to x-axis)
- RL simple shear: $[0,0,-1,0]$ (parallel to y-axis)
- RL simple shear: $[-\sin \theta \cos \theta, \cos^2 \theta, -\sin^2 \theta, \sin \theta \cos \theta]$ (in direction θ measured CCW from x-axis)
- LL simple shear: $[0,-1,0,0]$ (parallel to x-axis)
- LL simple shear: $[0,0,1,0]$ (parallel to y-axis)
- [Equal amounts of RL/LL simple shear and extension/convergence in all oblique examples following below...]
- Oblique RL extension: $[1,0,-1,0]$ (parallel to x-axis)
- Oblique RL extension: $[0,1,0,1]$ (parallel to y-axis)
- Oblique LL extension: $[1,0,1,0]$ (parallel to x-axis)
- Oblique LL extension: $[0,-1,0,1]$ (parallel to y-axis)
- Oblique RL convergence: $[-1,0,-1,0]$ (parallel to x-axis)
- Oblique RL convergence: $[0,1,0,-1]$ (parallel to y-axis)
- Oblique LL convergence: $[-1,0,1,0]$ (parallel to x-axis)
- Oblique LL convergence: $[0,-1,0,-1]$ (parallel to y-axis)
- Others?

Figure Captions

Figure 1. Directional derivatives for four gradient tensors that serve as a basis for the 4-dimensional space of 2×2 matrices. Each produces a simple flow pattern / tectonic style.

Figure 2. Directional derivatives for four more gradient tensors that also serve as a basis for the 4-dimensional space of 2×2 matrices. Again, each produces a simple flow pattern / tectonic style.

Figure 3. (a) Equal-area projection of the unit hemisphere in the 3-dimensional $[A, B, C]$ half-space. Colors and names indicate various selected tectonic styles listed in the text. Styles actually grade into each other as the boundaries of colored regions are approached. (b) Symbols added based on directional derivatives of the gradient tensor for the various styles. The

symbols in the inner ring have been oriented so that the maximum magnitude of the directional derivative (MMDD) directions, denoted by dashed lines, are vertical; the minimum (mMDD) value is zero for all styles in this ring. The symbols in the outer ring have equal MMDD values in all directions, as can be guessed from the symmetry of the symbols.

Figure 4. Equal-area plot and map view showing gradient tensors with magnitudes greater than **0.25 microstrain**. Not surprisingly, most tensors with such magnitudes are located along the San Andreas fault in California. Note also a region of light blue north of the Mendocino Triple Junction in California exhibiting mostly clockwise vorticity, and a small green region in Mexico of oblique RL extension (suspicious given its proximity to the map edge). The black dots mark the styles at individual grid points in the gridded data set.

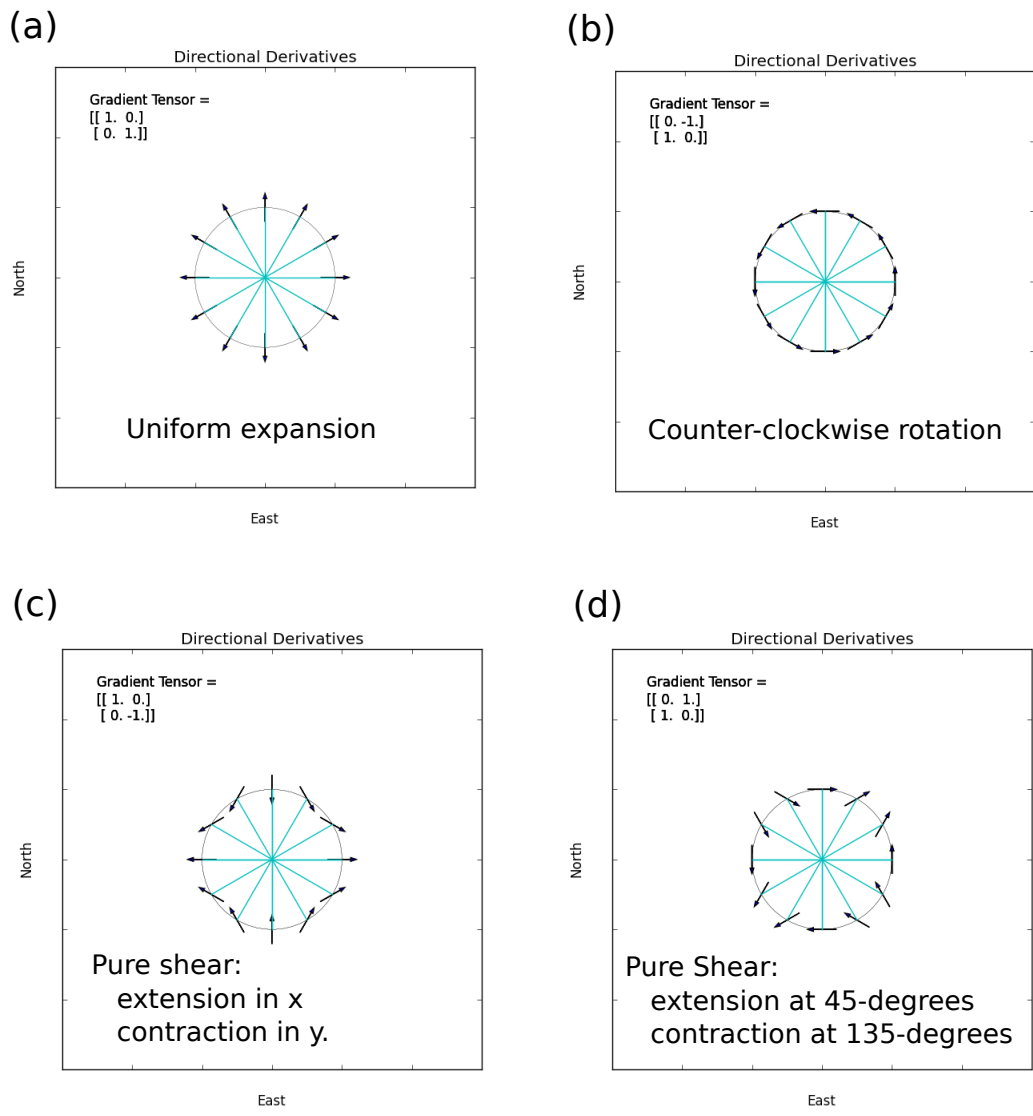
Figure 5. Same region as Figure 4 showing gradient tensors with magnitudes greater than **0.04 microstrain**. Note regions of oblique RL convergence along the coasts north of the Mendocino Triple Junction, changing in northwest Washington to convergence, oblique LL convergence, and LL shear in the vicinity of Vancouver Island.

Figure 6. Grid of selected data from Snay et al. (2016) excluding only regions with no data within 100 km. No attempt has been made in this plot to blank out areas with low intensities of deformation, or to attempt to propagate uncertainties. MMDD/mMDD deformation symbols are not scaled by the magnitude of the gradient tensor. Black lines in the symbols are for MMDD, white lines for the mMDD part. The LL shear colors showing in Utah and southern Nevada along the margin of the Colorado Plateau coincides with the Pahranagat shear zone, a SW trending LL zone accommodating westward extension in the Basin Range province (per Ray Wells). Note also the LL simple shear on Vancouver Island opposite the Nootka fracture zone offshore.

Figure 7. Delaunay triangulation of selected data from Snay et al. (2016). For this figure, we have colored only those triangles with 4 or fewer styles in the suite of styles generated by consideration of the uncertainties in the observations.

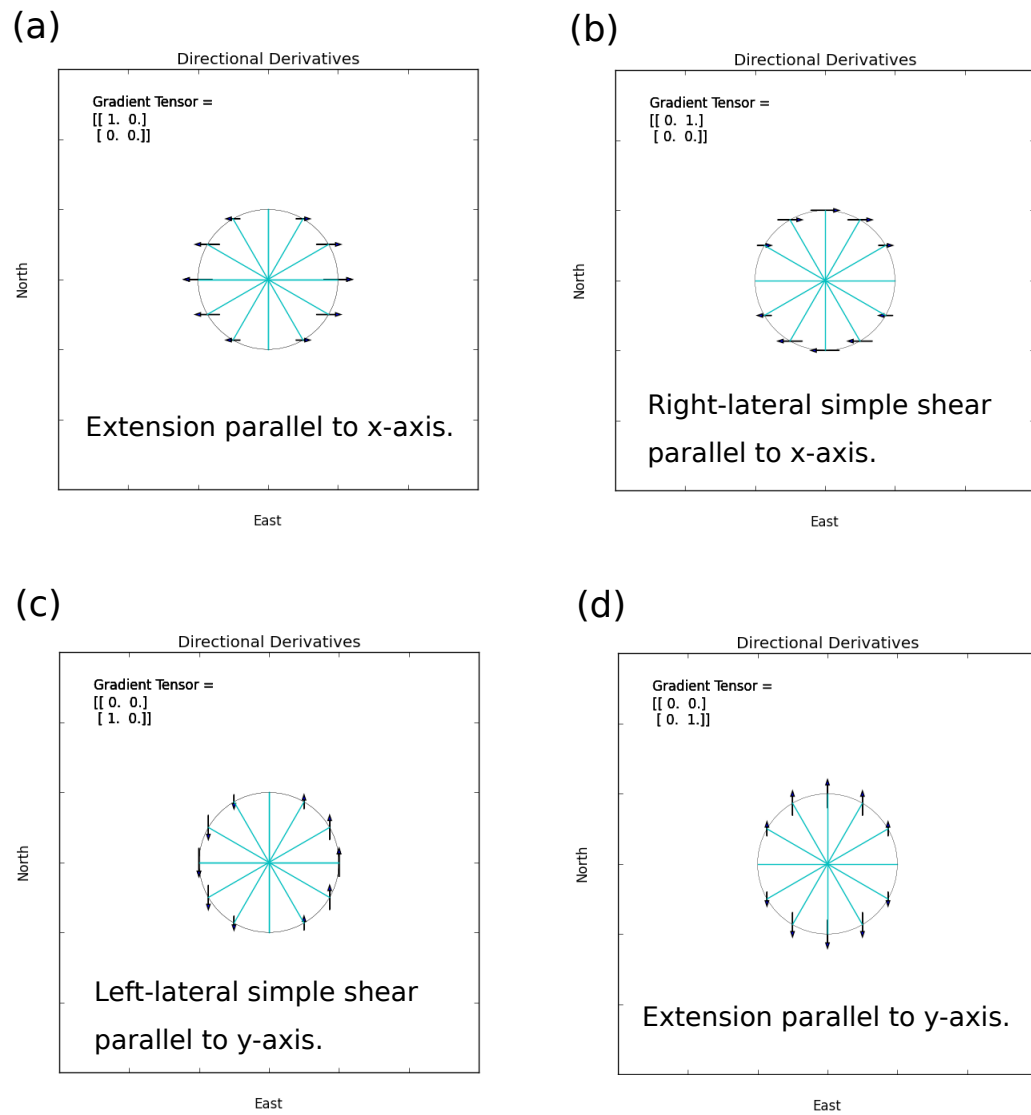
Figure 8. Ignores the change in scale (dilatation) style dimension and uses a different coloring of styles than in previous figures — more continuous than discrete — across a horizontal cross-section of the [A,B,C] upper hemisphere. Shading is intended to indicate the magnitude of the deformation, with the idea that small deformations are less likely to yield significant style picks. MMDD/mMDD symbols are scaled to the magnitude of the deformation. Data are from the WUS compilation of velocities of Rob McCaffrey.

Figure 9. Ignores the rotation (vorticity) style dimension and uses a different coloring of styles than in previous figures across a vertical cross-section of the [A,B,C] upper hemisphere. Shading is intended to indicate the magnitude of the deformation, with the idea that small deformations are less likely to yield significant style picks. Data are from the WUS compilation of velocities of Rob McCaffrey.



Directional derivatives at 30-degree intervals for four gradient tensors forming a basis for 2x2 matrices.

Figure 1



Directional derivatives at 30-degree intervals for four gradient tensors forming a basis for the space of 2x2 matrices.

Figure 2

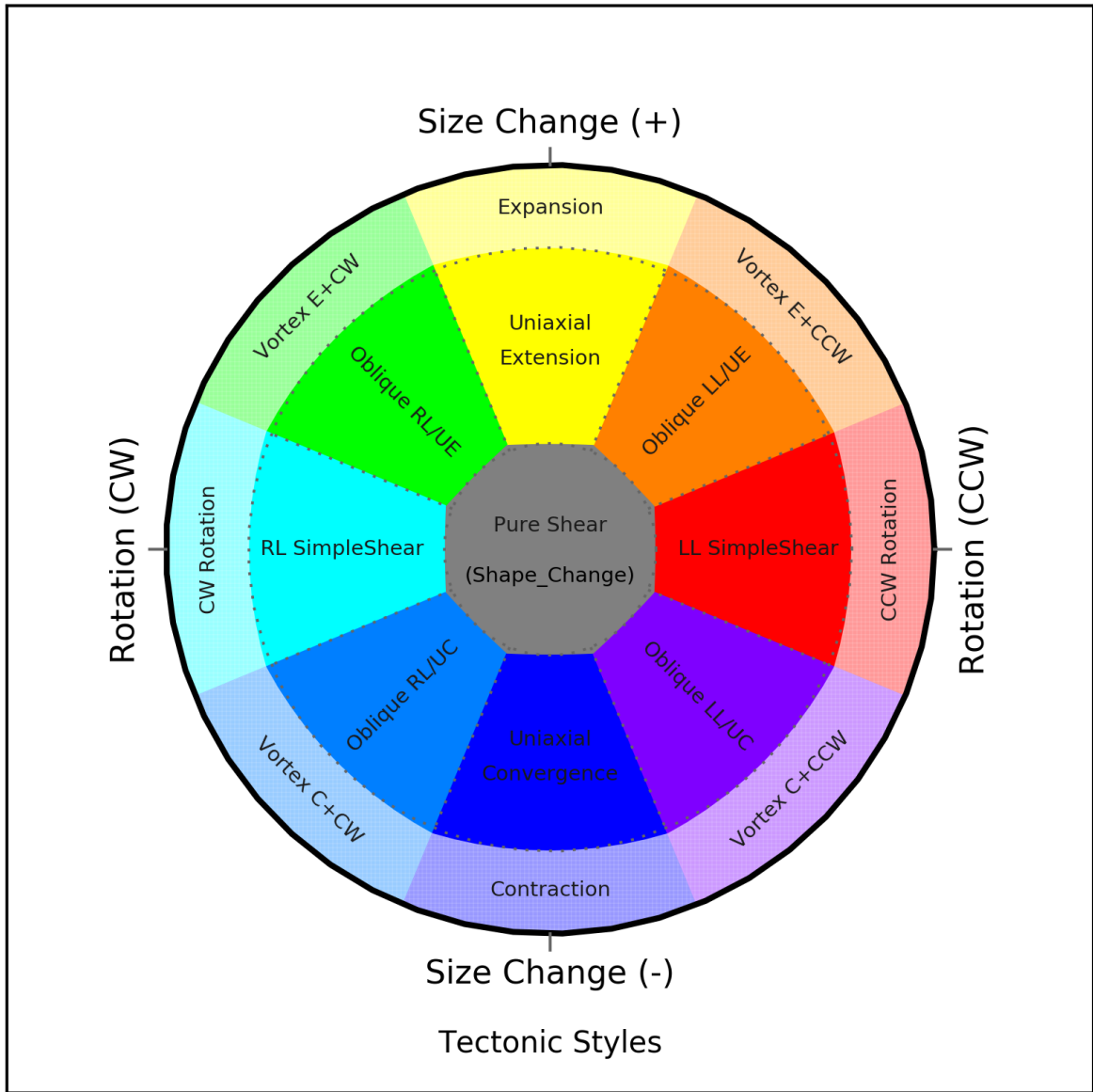


Figure 3a

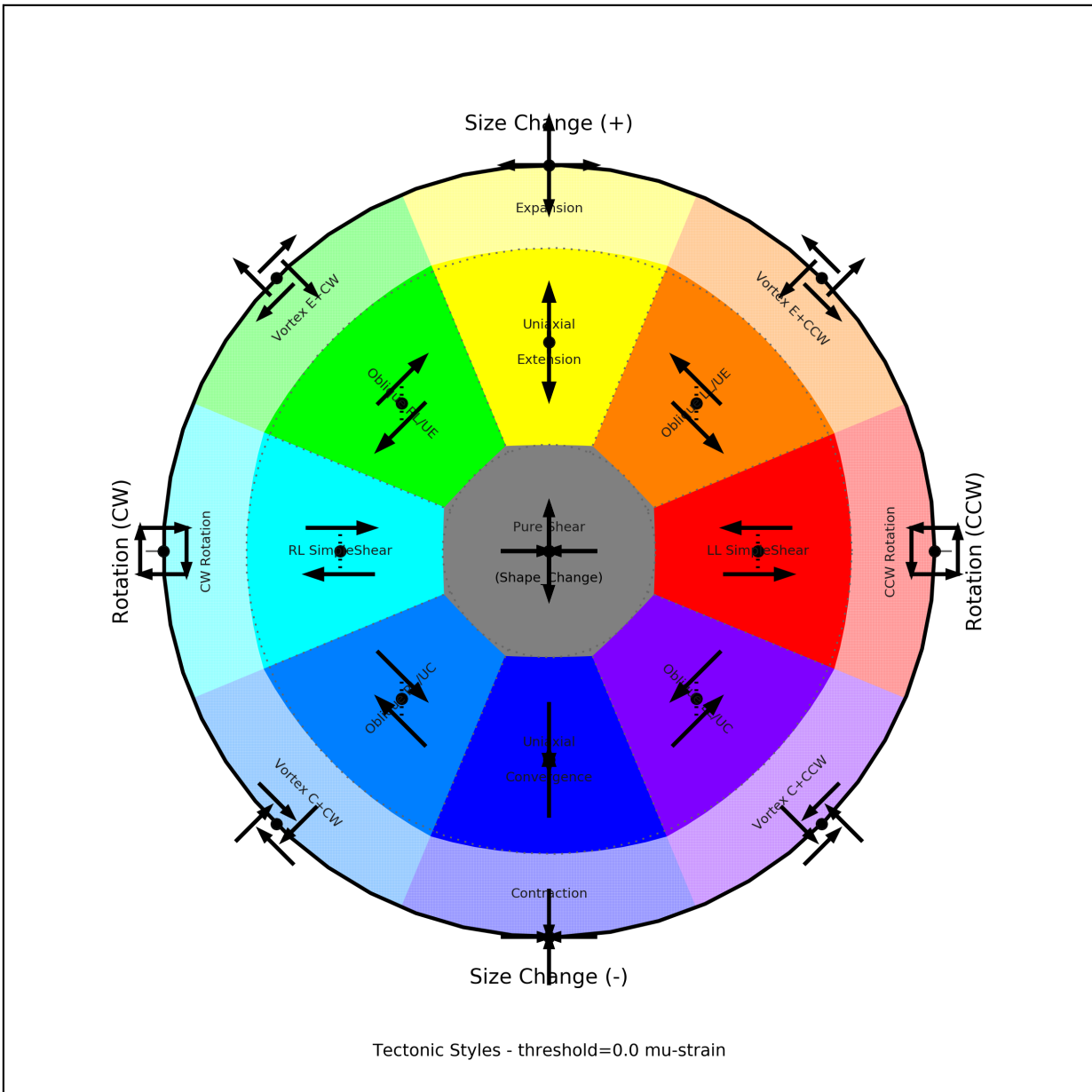


Figure 3b

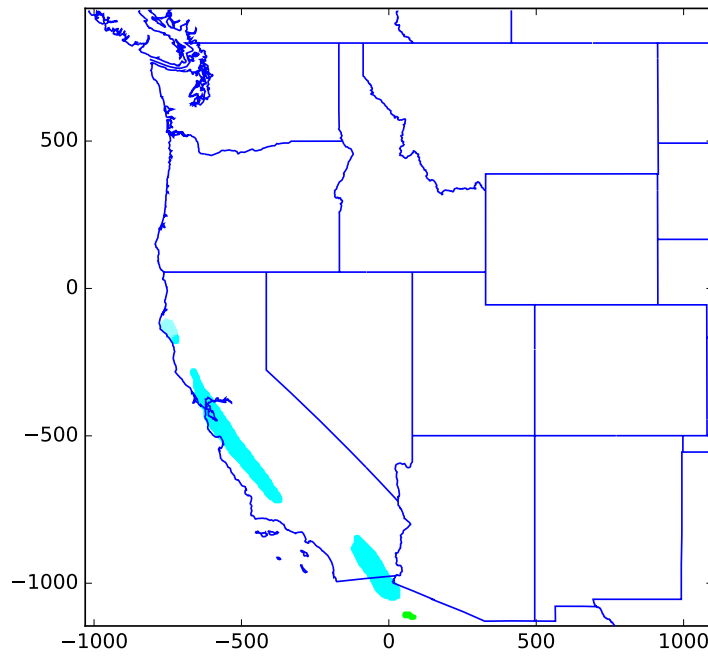
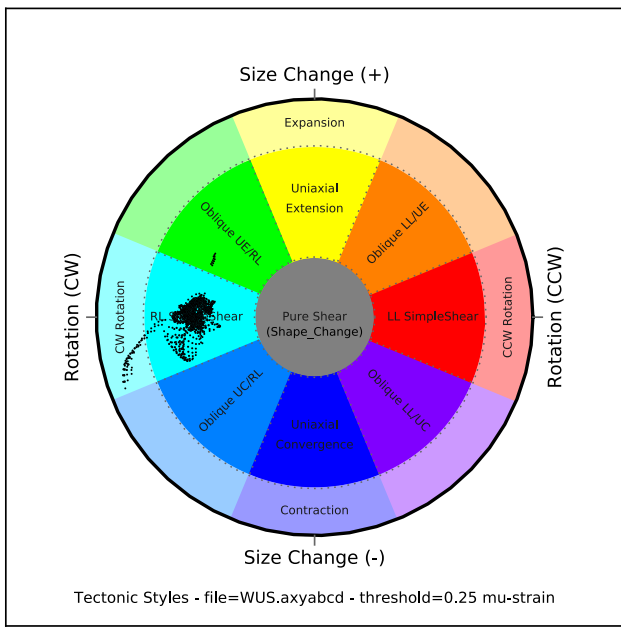


Figure 4

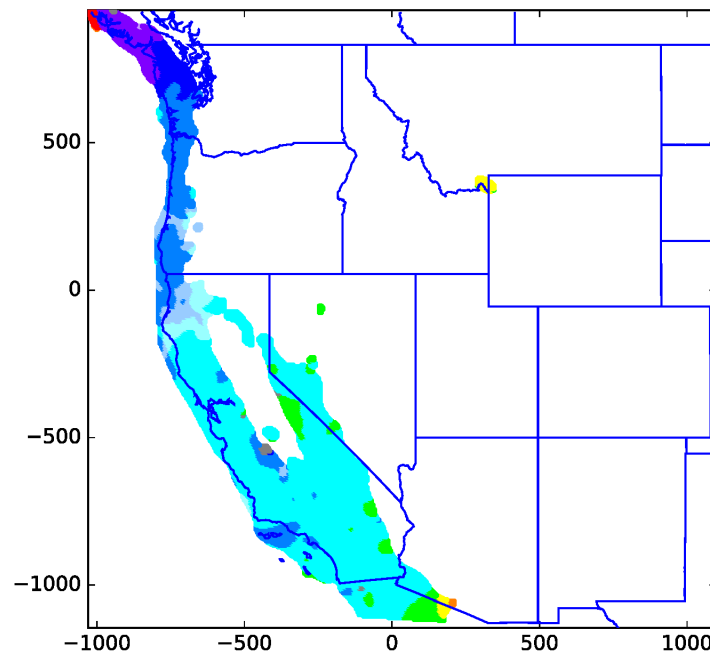
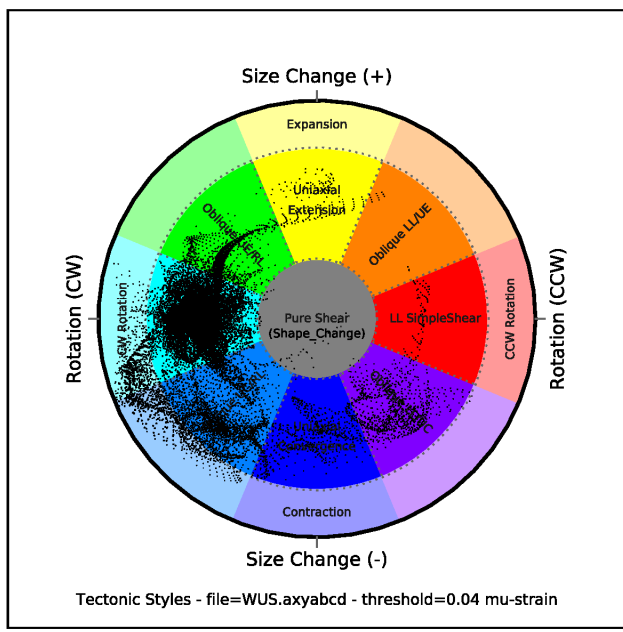


Figure 5

Style Codes with MMDD/mMDD Symbols

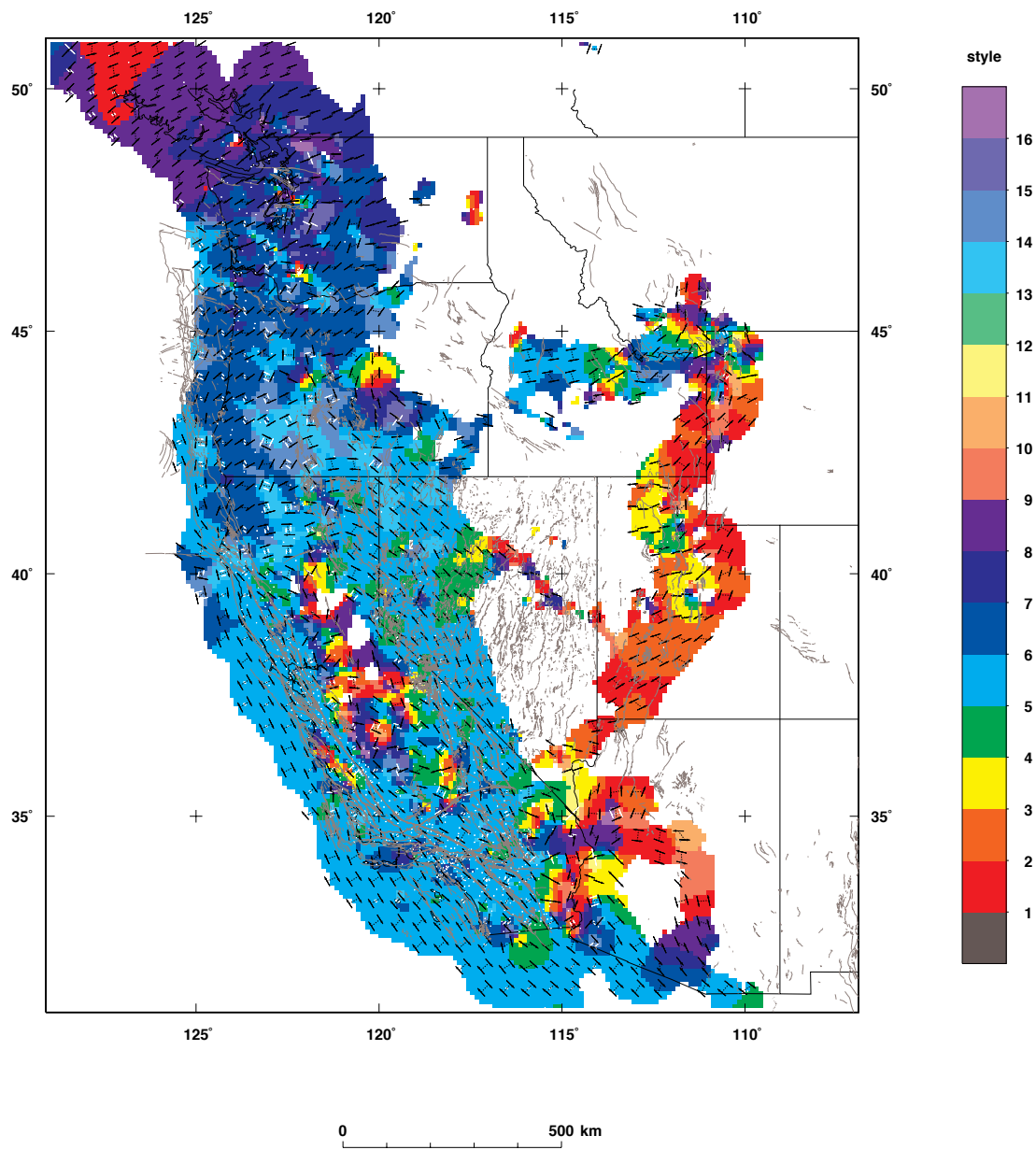


Figure 6

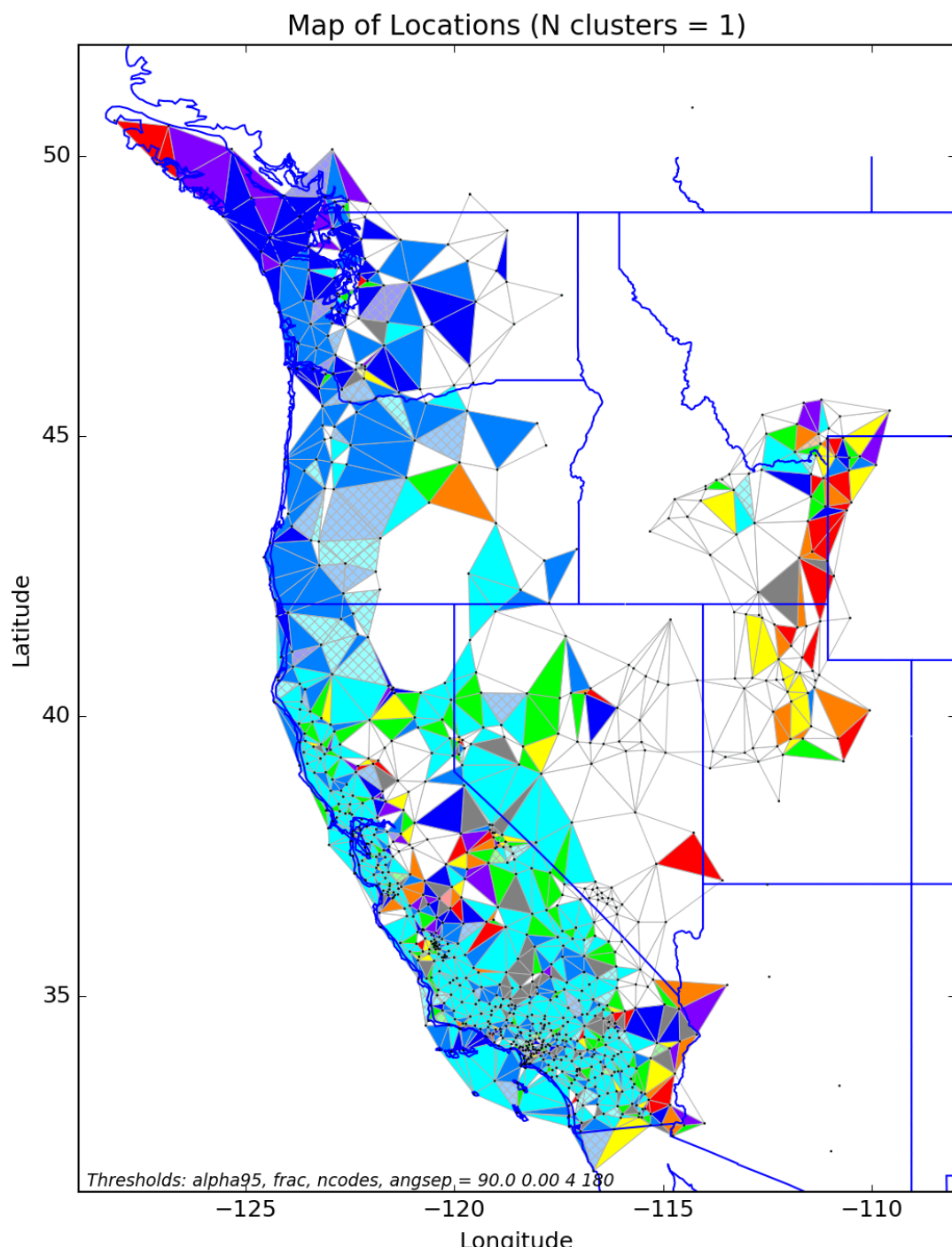


Figure 7

Deformation Style - Rotation and Shear (Ignoring Dilatation)

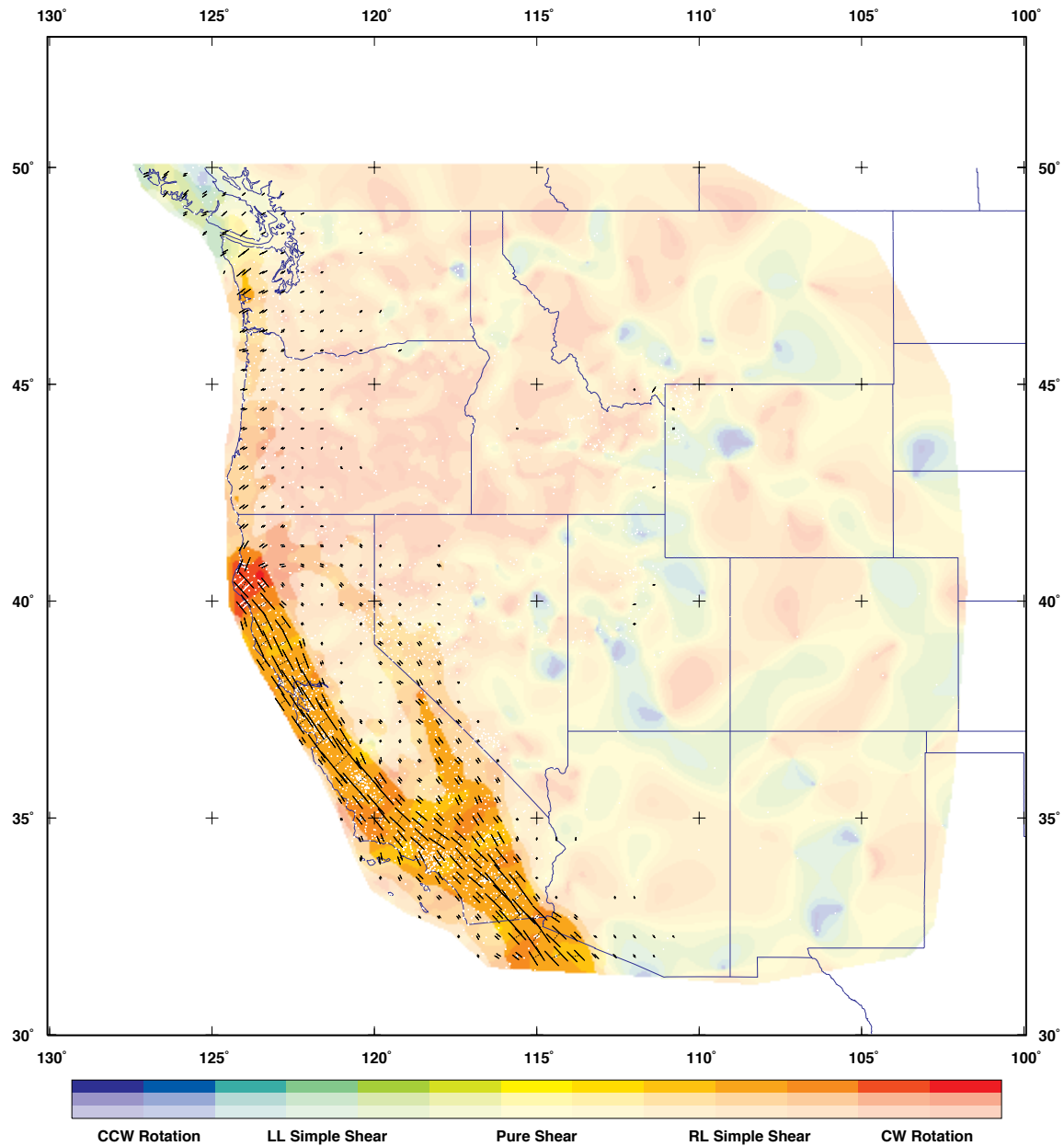


Figure 8

Deformation Style - Dilatation and Shear (Ignoring Rotation)

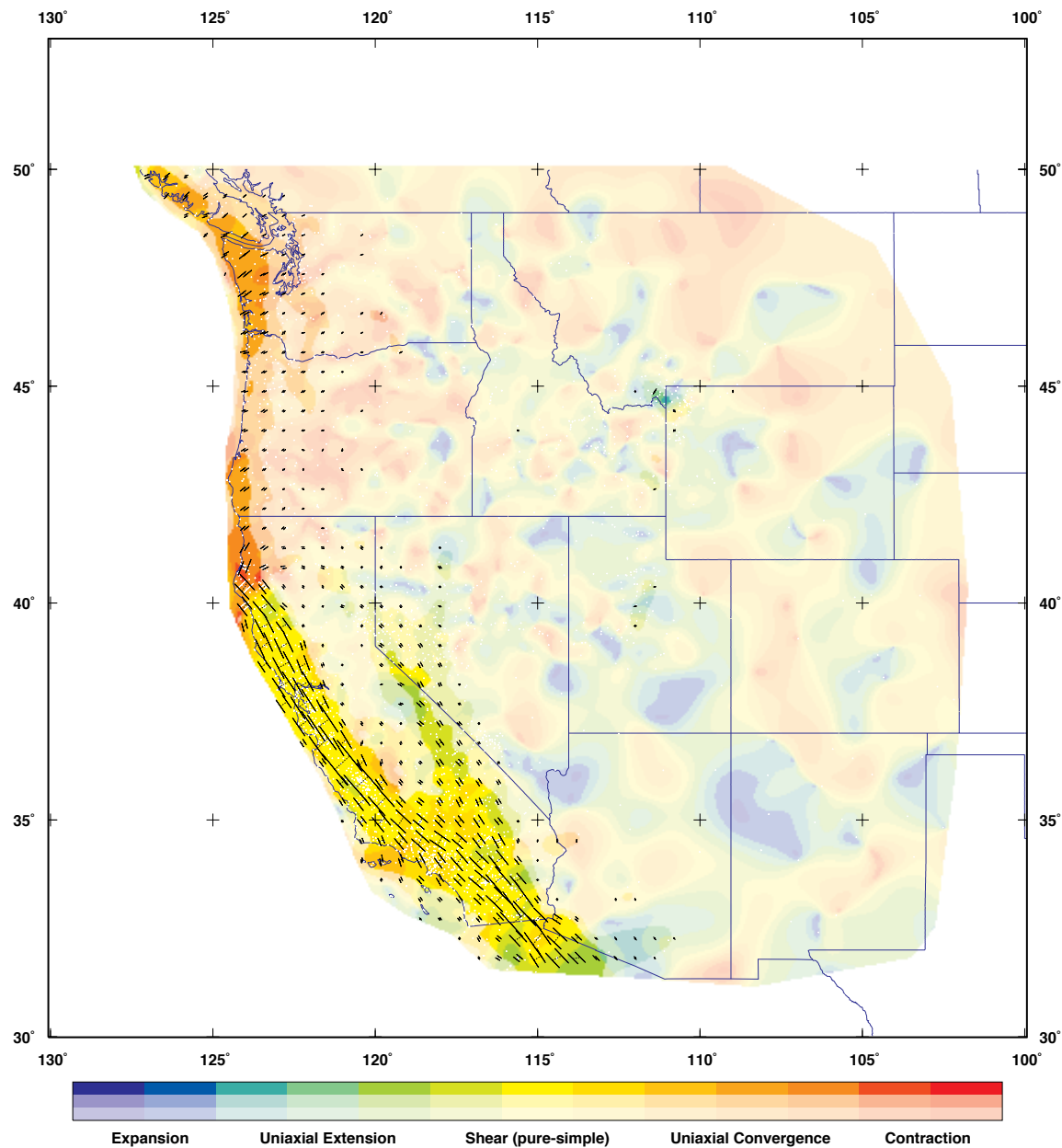


Figure 9